

Ferroelectricity in multiferroic magnetite Fe_3O_4 driven by noncentrosymmetric $\text{Fe}^{2+}/\text{Fe}^{3+}$ charge-ordering: First-principles study

Kunihiko Yamauchi, Tetsuya Fukushima, and Silvia Picozzi*

CASTI Regional Laboratory, Consiglio Nazionale delle Ricerche-Istituto Nazionale di Fisica della Materia (CNR-INFN),
67100 L'Aquila, Italy

(Received 4 April 2009; published 18 June 2009)

By means of first-principles simulations, we unambiguously show that improper ferroelectricity in magnetite in the low-temperature insulating phase is driven by charge-ordering. An accurate comparison between monoclinic ferroelectric Cc and paraelectric $P2/c$ structures shows that the polarization arises because of “shifts” of electronic charge between octahedral Fe sites, leading to a noncentrosymmetric $\text{Fe}^{2+}/\text{Fe}^{3+}$ charge-ordered pattern. Our predicted values for polarization, in good agreement with available experimental values, are discussed in terms of point-charge dipoles located on selected Fe tetrahedra, pointing to a manifest example of electronic ferroelectricity driven by charge rearrangement.

DOI: [10.1103/PhysRevB.79.212404](https://doi.org/10.1103/PhysRevB.79.212404)

PACS number(s): 75.50.Gg, 77.80.-e, 77.84.Bw

“Improper multiferroics”^{1–5} are attractive multifunctional materials where magnetism and ferroelectricity are strongly coupled. They can be classified according to different driving forces, which primarily break the spatial inversion symmetry paving the way to ferroelectricity: (1) spin order, (2) charge order (CO), and (3) orbital order. In this brief report, we will focus on the second group where LuFe_2O_4 has emerged as a prototype.⁶ However, recently Fe_3O_4 has been also suggested as a ferrimagnet with ferroelectricity being induced by charge-ordering,⁷ which would depict magnetite as the first multiferroic known to mankind. Fe_3O_4 shows the well-known first-order metal-insulator (Verwey) transition at $T_V \sim 120$ K below which the crystal structure changes from cubic $Fd\bar{3}m$ to monoclinic structure and $\text{Fe}^{2+}/\text{Fe}^{3+}$ charge-ordering is observed at the Fe B sites in the inverse-spinel AB_2O_4 lattice.^{8,9} Earlier experiments¹⁰ suggested Fe_3O_4 to show a spontaneous polarization at low temperatures, with the structure possibly undergoing a transition from monoclinic to triclinic symmetry.¹¹ However, up to date the physical mechanism underlying the rising of ferroelectricity is largely unknown. Khomskii⁷ has suggested that ferroelectric (FE) polarization is caused by a combination of site-centered and bond-centered charges between $\text{Fe}^{2+}/\text{Fe}^{3+}$ ions in the CO B-site Fe_4 -tetrahedron pattern. His model, based on the structure of Ref. 8 assumes each tetrahedron to show a “3:1” CO arrangement (three Fe^{2+} and one Fe^{3+} ions in a tetrahedron, or viceversa), at variance with Anderson’s criterion,¹² where each tetrahedron shows a “2:2” pattern (two Fe^{2+} and two Fe^{3+} ions). The 2:2 arrangement was found from density functional theory (DFT) (Ref. 13) on the cubic $Fd\bar{3}m$ structure, distorted by X_3 phonon mode. Moreover, the 3:1 arrangement was recently obtained within DFT (Refs. 13–15) on a monoclinic $P2/c$ structure. In addition, a mixed CO pattern (25% of 2:2 and 75% of 3:1 tetrahedra) was suggested to occur in a base-centered monoclinic Cc structure.¹⁶ Our DFT results, in agreement with Ref. 16, predict the Cc structure to be the ground state consistently with recent results from resonant x-ray scattering.¹⁷ As discussed in Ref. 16 and 18, the Cc symmetry is stabilized by a delicate balance of different effects: Coulomb repulsion, entropy,¹² Fermi-surface nesting¹⁹ leading to a [001] charge-density

wave (CDW),¹⁸ oxygen breathing modes,²⁰ etc.

Recent experimental data showing real-time FE switching in magnetite epitaxial thin films were found to be in good agreement with our DFT calculations for the polarization \mathbf{P} in the Cc FE structure.²¹ In this brief report, we focus on the proof of charge-ordering as the microscopic origin of ferroelectricity in Fe_3O_4 , by comparing two monoclinic $P2/c$ and Cc -lattice structures. Since the $P2/c$ structure shows inversion symmetry, the total \mathbf{P} must cancel out so that at most antiferroelectricity may occur; on the other hand, the Cc structure is ferroelectrically active due to the lack of centrosymmetry.

Electronic structure calculations were performed using the “Vienna *ab initio* simulation package (VASP),”²² where the projector-augmented-wave potentials, the generalized gradient approximation to the exchange-correlation potential²³ plus an effective on-site Coulomb interaction U were used.²⁴ In order to compare the total energies, the FE polarization and other relevant properties, we used for both paraelectric (PE) $P2/c$ and FE Cc states—the primitive cell of the base-centered monoclinic Cc lattice (with 112 atoms/cell) and experimental lattice parameters. Since the difference in experimental lattice constants between the PE and FE phases is $\sim 0.1\%$, the same lattice parameters in both unit-cells were used. The polarization vector \mathbf{P} is described with the conventional lattice vectors (a, b, c) . Internal atomic coordinates were optimized in both $P2/c$ and Cc starting from experimental Wyckoff parameters.^{8,20} The conventional atomic positions of the Cc lattice were displaced by $(-1/8, 0, 0)$ to fit into the $P2/c$ structure, so as to have the pseudoinversion center at $(0, 0, 0)$. We focus on the $P2/c$ and Cc structures since they are both proposed in diffraction experiments^{8,20} and show the lowest DFT total energies compared to other proposed symmetries, i.e., $Pmca$ and $Pmc2_1$.¹⁶ Note that the base-centered monoclinic lattice of $Cc(a=b \neq c, \alpha \neq \beta \neq \gamma \neq 90^\circ)$ is almost identical to a triclinic lattice (experimentally suggested as the FE state), the only difference being the $a=b$ condition. A cutoff energy of 400 eV for plane waves, $4 \times 4 \times 2$ Monkhorst-Pack k -point grid in the Brillouin zone, a threshold of atomic forces of 0.03 eV/Å were used. An effective Coulomb energy

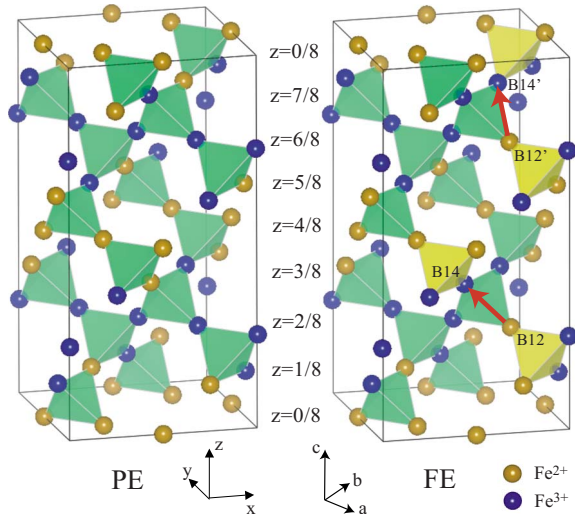


FIG. 1. (Color online) Ionic structure of Fe octahedral sites in $P2/c$ (left) and Cc (right) cells. Orange and blue balls show Fe^{2+} and Fe^{3+} ions, respectively. Fe_4 tetrahedra of 2:2 and 3:1 CO patterns are highlighted by yellow and green color planes, respectively. Electric dipole moments caused by charge shifts are indicated by red arrows. The lattice vectors in the primitive unit cell (x, y, z) and the conventional cell (a, b, c) are indicated.

$U=4.5$ eV and an exchange parameter $J=0.89$ eV (as in Ref. 15) were used for Fe- d states, although some calculations with different values of U were performed (see below). Fe- $3p^63d^64s^2$ and O- $2s^22p^4$ electrons were treated as valence states. For Fe ions, the ferrimagnetic configuration was considered, with all octahedral Fe sites as spin-up sites and all tetrahedral Fe sites as spin-down sites. Spin-orbit coupling was neglected.

In terms of relevant structural and electronic properties, our results are similar to the previous study by Jeng *et al.*,¹⁶ so in this brief report we will focus only on FE properties.

As shown in Fig. 1, octahedral Fe sites are located in xy planes with $z=i/8$ ($i=0\dots7$). The PE state has $\{E, C_{2b}+(0,0,1/2), I, \sigma_{2b}+(0,0,1/2)\}$ symmetries and the FE state has $\{E, \sigma_{2b}+(0,0,1/2)\}$ symmetries in a conventional base-centered monoclinic cell so that there are two equivalent atoms (cf. B12 and B12' sites in Fig. 1). Note that (i) the mirror symmetry along with the translation vector forbids any net polarization along b and finite \mathbf{P} is allowed only along the a and c directions; (ii) the translation vector is relevant for the CDW stabilization and for opening the energy gap.¹⁸ As discussed in Ref. 15 and 16, the PE state shows entirely a 3:1 tetrahedron CO arrangement whereas the FE state shows a mixed pattern. The difference between the two CO distributions (see Fig. 2 for the $P2/c$ and Fig. 3 for the Cc) can be understood when assuming a charge “shift” from B12 to B14 site and in the upper part of the cell, from B12' to B14', all the other sites keeping their valence state. Each charge shift creates two 2:2 CO tetrahedra, so as to form four 2:2 tetrahedra (cf. Fig. 1). The resulting CO pattern lacks inversion symmetry, therefore allowing FE polarization. The CO rearrangement implies a change in the local breathing mode of O ions, which are driven away (attracted) by the substituted $\text{Fe}^{2+}(\text{Fe}^{3+})$ ion at B12 (B14) site,

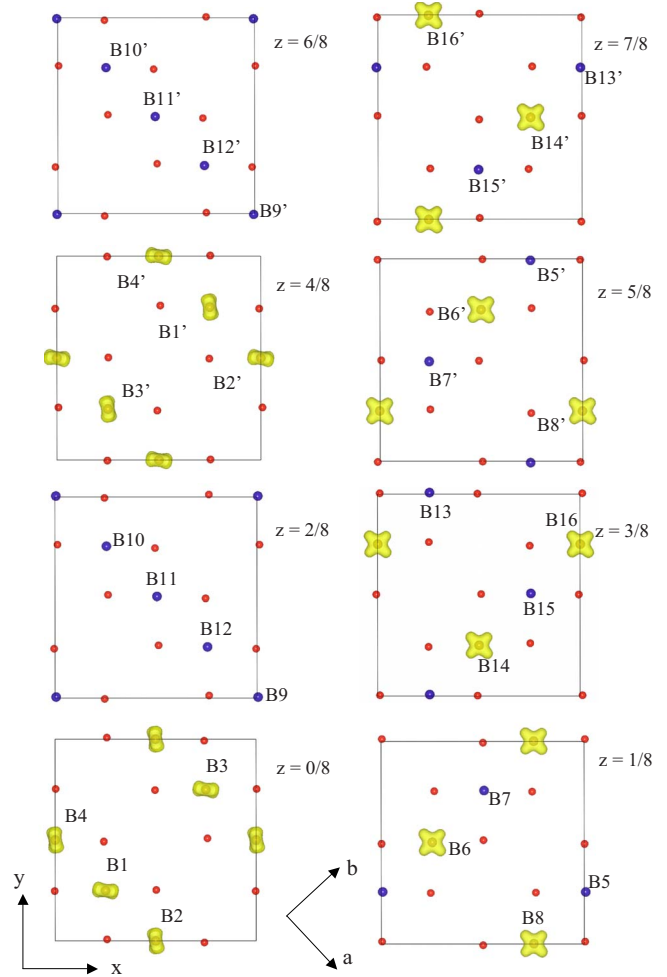


FIG. 2. (Color online) Charge/orbital ordering of Fe minority t_{2g} states in PE configuration. Blue (orange) large balls show $\text{Fe}^{3+}(\text{Fe}^{2+})$ ions. Red small balls show O ions.

with a displacement of ~ 0.1 Å (cf. small black arrows in Fig. 3). Similarly, upon charge shifts of the Fe t_{2g} electron between sites, some of the Fe^{3+} ions (at B9 and B11 sites) move toward the Fe^{2+} ions, maybe reminiscent of Khomskii’s mixed bond-/site-centered charge mechanism.⁷ However, as far as ferroelectricity is concerned when focusing on a Fe chain along $[100]$, these movements average out so as not to give a net contribution to \mathbf{P} .

As for calculated \mathbf{P} (cf. Table I), the Berry phase approach²⁵ predicts quite a large polarization (at least compared to other improper multiferroics),^{1,2} its direction lying in the ac -mirror plane. As noted previously,²¹ the DFT results are in excellent agreement with recently reported experimental values for magnetite thin films ($P \sim 5.5$ $\mu\text{C}/\text{cm}^2$ in the ab plane with the c component not measured) as well as with earlier experiments on single crystals:¹⁰ $P_a=4.8$ $\mu\text{C}/\text{cm}^2$ and $P_c=1.5$ $\mu\text{C}/\text{cm}^2$.

To deepen our analysis, we compare the value of $\mathbf{P}_{\text{Berry}}$ with the value estimated from a point charge model, (\mathbf{P}_{PCM}), assuming the nominal valence for every ion, i.e., “full” charge disproportionation, i.e., 2+ and 3+ for charge-ordered Fe, 2− for O as well as with a simple model (\mathbf{P}_{dip}) where we summed up the two dipole moments located at sites where

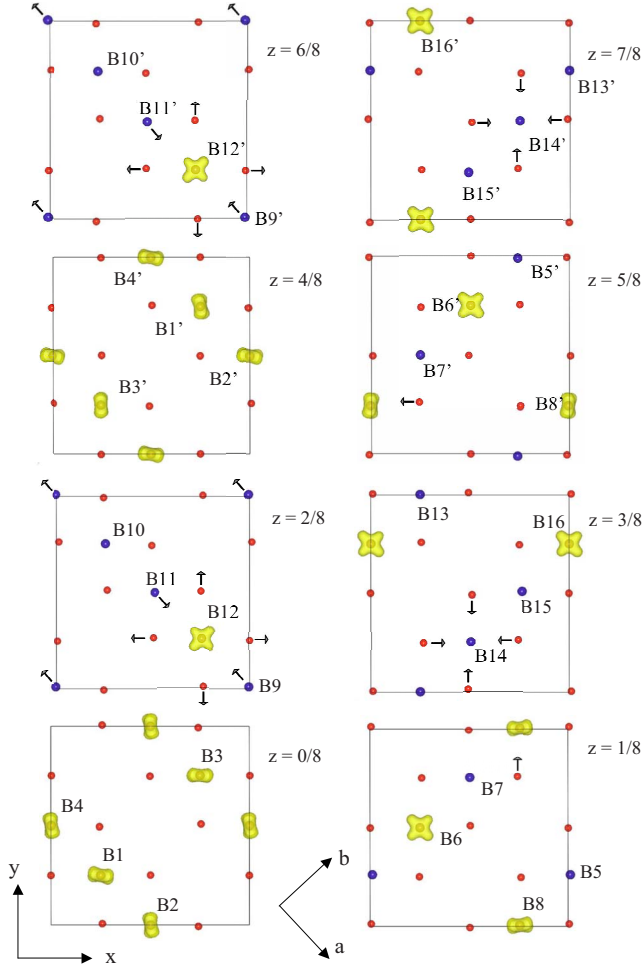


FIG. 3. (Color online) Charge/orbital ordering of Fe minority t_{2g} states in FE configuration (notation as in Fig. 2). Black arrows show atomic displacements with respect to the PE reference state.

charge-shifting occurs (i.e., from B12 to B14 site) with nominally one electron (see red arrows in Fig. 1). The consistency of these values, shown in Table I, implies two important facts: (i) \mathbf{P} is induced largely by the CO rearrangement (i.e., charge shifts at few sites) but not much by the ionic displacements, as evident by the similarity between \mathbf{P}_{PCM} and \mathbf{P}_{dip} ; (ii) since the Berry-phase value is equivalent to the sum of Wannier-function (WF) centers,²⁵ the similarity between $\mathbf{P}_{\text{Berry}}$ and \mathbf{P}_{PCM} suggests the WF of Fe- d electron to be mostly centered at the ionic sites, no matter how the WF is delocalized and hybridized with surrounding O- p orbitals.

Our picture based on the WF centers is also confirmed by the results of $\mathbf{P}_{\text{Berry}}$ values upon varying the U Coulomb parameter. As shown in Table II, upon increasing U and keeping the atomic configuration fixed to that obtained for $U=4.5$ eV, the charge separation between Fe²⁺ and Fe³⁺ is

TABLE I. \mathbf{P} along a , b , and c axes (in $\mu\text{C}/\text{cm}^2$), calculated with different approaches (see text).

$\mathbf{P}_{\text{Berry}}$	\mathbf{P}_{PCM}	\mathbf{P}_{dip}
(-4.41, 0, 4.12)	(-4.20, 0, 5.27)	(-4.05, 0, 5.73)

TABLE II. Charge separation (cs, i.e., difference of d charges between Fe²⁺ and Fe³⁺ ions in the atomic sphere with 1 Å: radius) and the corresponding FE $\mathbf{P}_{\text{Berry}}$ (in $\mu\text{C}/\text{cm}^2$) vs Coulomb repulsion U (J is fixed to 0.89 eV).

$U(\text{eV})$	4.5	6.0	8.0
cs	0.17	0.23	0.30
$\mathbf{P}_{\text{Berry}}$	(-4.41, 0, 4.12)	(-4.42, 0, 4.81)	(-4.33, 0, 5.07)

enhanced. Note that the value of \mathbf{P} does not change rapidly with U , suggesting the centers of the WF not to move significantly far from the Fe²⁺ for all U values. Also, in the limit of extremely large U , we expect a “full” charge disproportionation to occur, causing $\mathbf{P}_{\text{Berry}}$ to become progressively closer to \mathbf{P}_{PCM} (as confirmed by Table II).

For further insights, an “adiabatic” path is set up to connect the PE and FE state by displacing all ions linearly with a scaling parameter λ (i.e., $\lambda=1$ for full FE displacements and $\lambda=0$ for the initial PE structure). The FE structure with opposite \mathbf{P} was built starting from the PE structure and with $\lambda=-1$, i.e., with displacements opposite to the structure considered so far. By analogy with the above discussion for positive λ values, two charge shifts between B10 and B6 (B10' and B6') occur as a transition from the PE to the “negative” FE phase. The charge separation (cs) is calculated by comparing the “muffin-tin” charge on the sites where the shift occurs in going from PE to FE (i.e., B12–B14 sites

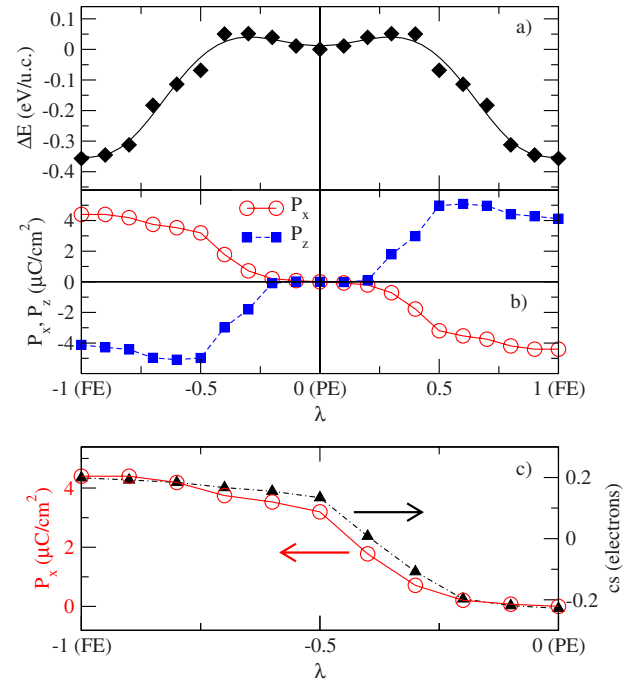


FIG. 4. (Color online) (a) Total energy per unit cell (ΔE , with the black line as a guide to the eye) and (b) Polarization (P_x and P_z components) along the adiabatic path between FE structures with opposite \mathbf{P} through the PE structure vs the scaling parameter λ (see text). (c) Polarization P_x (left scale on the y axis, see empty red circles) and charge separation (right scale on the y axis and filled black triangles) along the FE ($\lambda=-1$) to PE ($\lambda=0$) path.

when $\lambda > 0$). The results are reported in Fig. 4. The total energy shows a double valley structure, typical for ferroelectricity, with a deep global minimum at the FE state along with a very shallow local minimum at the PE state. In going from the PE to the FE state, we show that the charge shift rather suddenly occurs around $\lambda = 0.5$, when \mathbf{P} is strongly enhanced and the total energy reduced²⁶ [cf. Figs. 4(a) and 4(b)]. Moreover, the origin of ferroelectricity as driven by charge rearrangements on different sites is clearly confirmed by the trend of P_x closely following that of c_s along the path [cf. Fig. 4(c)].

In summary, we have shed light on the microscopic origin of ferroelectric polarization in insulating magnetite by analyzing the differences between two charge-ordered states: the $P2/c$ PE state and the Cc FE state. Ferroelectricity is in-

duced by a noncentrosymmetric charge-ordering and the polarization is primarily caused by local dipoles at selected octahedral sites, pointing to a picture of ferroelectricity mostly based on localized “charge shifts.” Our calculations show that Fe_3O_4 can be considered as a prototypical case of charge-order driving multiferroicity with relatively large values for the electric polarization.

We thank Daniel Khomskii for his careful reading of the manuscript. The research leading to these results has received funding from the European Research Council under the EU Seventh Framework Programme (FP7/2007-2013)/ERC Grant Agreement No. 203523. Computational support from Caspur Supercomputing Center (Rome) is gratefully acknowledged.

*silvia.picozzi@aquila.infn.it

- ¹S. W. Cheong and M. Mostovoy, *Nature Mater.* **6**, 13 (2007).
- ²T. Kimura, T. Goto, H. Shintani, K. Ishizaka, T. Arima, and Y. Tokura, *Nature (London)* **426**, 55 (2003).
- ³D. V. Efremov, J. van der Brink, and D. I. Khomskii, *Nature Mater.* **3**, 853 (2004).
- ⁴S. Picozzi, I. A. Sergienko, K. Yamauchi, B. Sanyal, and E. Dagotto, *Phys. Rev. Lett.* **99**, 227201 (2007).
- ⁵K. Yamauchi and S. Picozzi, *J. Phys.: Condens. Matter* **21**, 064203 (2009).
- ⁶N. Ikeda, H. Ohsumi, K. Ohwada, K. Ishii, T. Inami, K. Kakurai, Y. Murakami, K. Yoshii, S. Mori, Y. Horibe, and H. Kito, *Nature (London)* **436**, 1136 (2005).
- ⁷D. Khomskii, *Bull. Am. Phys. Soc.* **A13**, 00006 (2007); J. van den Brink and D. I. Khomskii, *J. Phys.: Condens. Matter* **20**, 434217 (2008).
- ⁸J. P. Wright, J. P. Attfield, and P. G. Radaelli, *Phys. Rev. B* **66**, 214422 (2002).
- ⁹J. Schlappa, C. Schüßler-Langheine, C. F. Chang, H. Ott, A. Tanaka, Z. Hu, M. W. Haverkort, E. Schierle, E. Weschke, G. Kaindl, and L. H. Tjeng, *Phys. Rev. Lett.* **100**, 026406 (2008).
- ¹⁰K. Kato, S. Iida, K. Yanai, and K. Mizushima, *J. Magn. Magn. Mater.* **31-34**, 783 (1983).
- ¹¹C. Medrano, M. Schlenker, J. Baruchel, J. Espeso, and Y. Miyamoto, *Phys. Rev. B* **59**, 1185 (1999).
- ¹²P. W. Anderson, *Phys. Rev.* **102**, 1008 (1956).
- ¹³P. Piekarczyk, K. Parlinski, and A. M. Oleś, *Phys. Rev. B* **76**, 165124 (2007).
- ¹⁴I. Leonov, A. N. Yaresko, V. N. Antonov, M. A. Korotin, and V. I. Anisimov, *Phys. Rev. Lett.* **93**, 146404 (2004).
- ¹⁵H.-T. Jeng, G. Y. Guo, and D. J. Huang, *Phys. Rev. Lett.* **93**, 156403 (2004).
- ¹⁶H.-T. Jeng, G. Y. Guo, and D. J. Huang, *Phys. Rev. B* **74**, 195115 (2006).
- ¹⁷Y. Joly, J. E. Lorenzo, E. Nazarenko, J.-L. Hodeau, D. Mannix, and C. Marin, *Phys. Rev. B* **78**, 134110 (2008).
- ¹⁸J. P. Wright, J. P. Attfield, and P. G. Radaelli, *Phys. Rev. Lett.* **87**, 266401 (2001).
- ¹⁹A. Yanase and N. Hamada, *J. Phys. Soc. Jpn.* **68**, 1607 (1999).
- ²⁰J. M. Zuo, J. C. H. Spence, and W. Petuskey, *Phys. Rev. B* **42**, 8451 (1990).
- ²¹M. Alexe, M. Ziese, D. Hesse, P. Esquinazi, K. Yamauchi, T. Fukushima, S. Picozzi, and U. Gösele, *Adv. Mater.* (to be published).
- ²²G. Kresse and J. Furthmüller, *Phys. Rev. B* **54**, 11169 (1996).
- ²³J. P. Perdew, K. Burke, and M. Ernzerhof, *Phys. Rev. Lett.* **77**, 3865 (1996).
- ²⁴V. I. Anisimov, F. Aryasetiawan, and A. I. Lichtenstein, *J. Phys.: Condens. Matter* **9**, 767 (1997).
- ²⁵R. D. King-Smith and D. Vanderbilt, *Phys. Rev. B* **47**, 1651 (1993); R. Resta, *Rev. Mod. Phys.* **66**, 899 (1994).
- ²⁶At variance with monotonous increase in P_x vs λ , P_z shows a bump at $\lambda \sim 0.5$ and decreases up to $\lambda = 1.0$: this trend may come from partial cancellation of ionic and electronic contribution to \mathbf{P} for $0.5 < \lambda < 1$.